ACS APPLIED MATERIALS & INTERFACES

Research Article

www.acsami.org

Tailoring Properties of Cross-Linked Polyimide Aerogels for Better Moisture Resistance, Flexibility, and Strength

Haiquan Guo,*[,†] Mary Ann B. Meador,*[,‡] Linda McCorkle,[†] Derek J. Quade,[‡] Jiao Guo,[§] Bart Hamilton,[§] and Miko Cakmak[§]

[†]Ohio Aerospace Institute, 22800 Cedar Point Road, Cleveland, Ohio 44142, United States

[‡]NASA Glenn Research Center, 21000 Brookpark Road, Cleveland, Ohio, 44135, United States

[§]National Polymer Innovation Center, The University of Akron, Akron, Ohio, 44325, United States

ABSTRACT: Combinations of rigid and flexible aromatic diamines were used to tailor the properties of octa(aminophenyl)-silsesquioxane (OAPS) cross-linked polyimide aerogels. 2,2′-Dimethylbenzidine (DMBZ) or *p*-phenylenediamine (PPDA) was used in combination with the more-flexible diamine, 4,4′-oxydianiline (ODA). The amount of rigid diamine was varied from 0% to 100% of the total diamines in the backbone. The resulting aerogels vary in density, shrinkage, porosity, surface area, mechanical and thermal properties (depending on the type of diamine and the proportions of rigid diamine to flexible diamine used). Replacing ODA with PPDA increases shrinkage that occurs during gelation and processing, while increasing the DMBZ fraction decreases shrinkage. Replacing ODA with 50 mol % of DMBZ maintains the flexibility of thin films, while the moisture resistance of the aerogels is greatly improved.

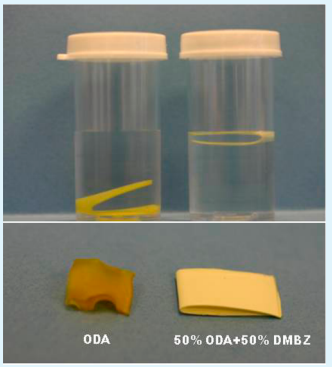

KEYWORDS: *polyimide, aerogel, mesoporous materials, cross-linking, insulation, polyoligomeric silsesquioxane*

INTRODUCTION

For aerospace applications, novel insulation materials are required with lower thermal conductivity, lighter weight, and higher use temperatures. Aerogels are an important class of porous solids exemplified by having very small pore sizes and very high porosity, making them superior thermal insulators, among other things.[1] Because silica aerogel monoliths are fragile and hygroscopic, they are limited in application, especially in extreme environments such as aerospace.[2] We are interested in developing aerogels with better mechanical and environmental stability for a variety of aeronautic and space applications, including insulation for extravehicular activity (EVA) suits for planetary surface missions[3] or inflatable structures such as habitats, flexible thermal protection systems (TPS) for inflatable aerodynamic decelerators for entry, descent, and landing operations,[4−6] and cryotank insulation for advance space propulsion systems.[7] Polymer-reinforced silica aerogels have improved compressive strength over native silica aerogels,[8] which makes them useful for insulating structures such as cryotanks. However, for applications such as EVA suits and flexible TPS, it is most desirable to have flexible insulation. Inflatable structures for entry, descent, and landing operations also require higher-temperature stability.

Previously reported cross-linked polyimide areogels are potential candidates for these applications, because they are stable up to 300−400 °C and thin films of the aerogels are flexible with good tensile properties.[9,10] These polyimide aerogels were fabricated from polyamic acid oligomers capped with an anhydride and cross-linked with either 1,3,5-triaminophenoxybenzene (TAB)[9] or octa(aminophenyl)-silsesquioxane (OAPS).[10] Both types of cross-linked aerogels, unlike other recently reported linear[11,12] polyimide aerogels, are produced with very little shrinkage during the processing. OAPS cross-linked aerogels have thermal conductivity comparable to silica aerogels of similar density (as low as 14 m W/(m K) in N_2) but are much stronger, with compressive modulus values ranging from 1 to 5 MPa. These aerogels were also recently tested in a layered insulation system meant to simulate heat loads for planetary re-entry, and were able to survive a laser heat flux load of 20 W/cm^2 for 90 s, while maintaining a 500 °C difference in temperature measured by thermocouples on the top-most and under the bottom-most insulation layers with a thickness of 6.5 mm.[13]

More recently, we have examined structure−property relationships of polyimide aerogels cross-linked with TAB, using two different dianhydrides and three different diamines in the backbone structure.[9] The best combination of properties was obtained for polyimide aerogels using 2,2′-dimethylbenzidine (DMBZ) and BPDA as the backbone structure. Shrinkage in this formulation was lowest among the TAB cross-linked polyimide aerogels but was higher compared to the OAPS cross-linked polyimide aerogels previously reported.[10] However, while the density was 26 % higher than the same formulation with OAPS cross-link, the compressive modulus

Received: July 16, 2012
Accepted: September 6, 2012
Published: September 6, 2012

Scheme 1. Synthesis of OAPS Cross-Linked Polyimide Aerogels

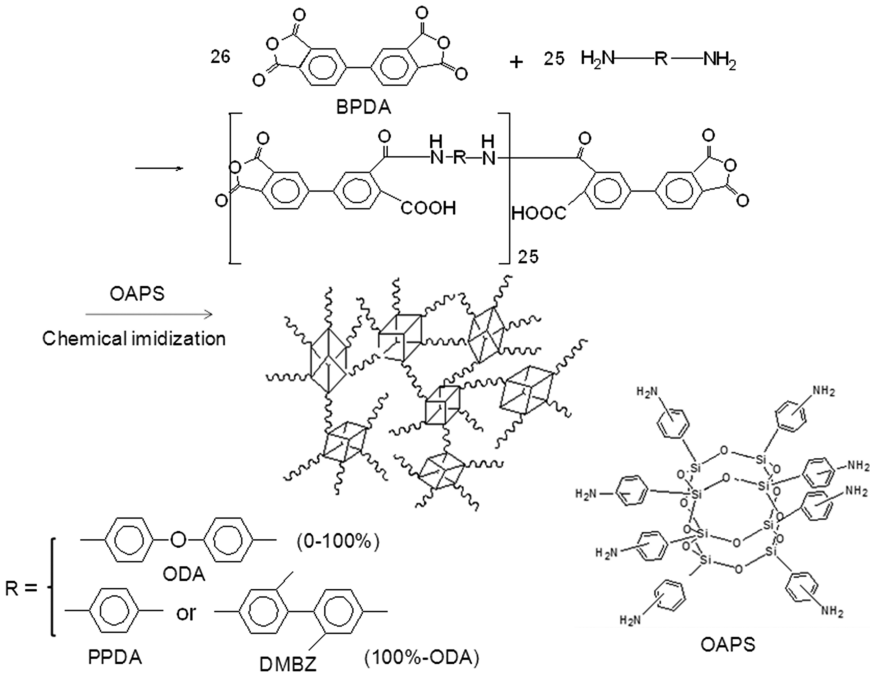

was a factor of four higher and surface areas measured by nitrogen sorption were also significantly increased. Other formulations studied with TAB cross-linking include those with *p*-phenylene diamine (PPDA) or 4,4′-oxydianiline (ODA) and BPDA in the polyimide backbone. Formulations made with PPDA exhibited the most shrinkage (40%−50%) during processing, but also were highest in thermal stability and glass-transition temperature. Finally, formulations made using ODA resulted in the most-flexible thin films. However, it was recently discovered that the oxygen links in the polyimide backbone make the aerogels susceptible to moisture. Water is readily absorbed into the aerogel and collapses the pore structure upon drying. In many applications where the insulation might be exposed to the elements, this is a fatal flaw. Thus, although each polyimide aerogel made with different dianhydride and diamine pairs has its own advantage, none of them can fulfill all the required properties, especially flexibility, low shrinkage, and resistance to moisture. Therefore, in this study, we wish to optimize the properties of the polyimide aerogels by using ODA in combination with either of the rigid diamines, PPDA or DMBZ. In this regard, DMBZ or PPDA are used to replace up to 100 mol % ODA to optimize the mechanical properties, thermal stability, resistance to moisture, and other properties of the polyimide aerogels, as shown in Scheme 1. It is also of interest to discern if the observed differences in properties (shrinkage, surface area, and mechanical properties) of OAPS vs. TAB cross-linked aerogels are due to different cross-linkers, different backbone structures, or both. As shown in Scheme 1, polyimide gels are obtained as previously described using chemical imidization at room temperature, using pyridine and acetic anhydride. The polyimide gels are then dried using CO_2 supercritical fluid extraction to produce polyimide aerogels. Fabrication of both molded cylinders and highly flexible, thin film polyimide aerogel monoliths are demonstrated. Mechanical properties, including compression and tensile measurements, and thermal properties of the aerogels are discussed and related to morphology and chemical structure.

EXPERIMENTAL SECTION

Materials. BPDA and ODA were purchased from Chriskev, Inc. (Lenexa, KS, USA). DMBZ and PPDA were purchased from Omni Specialty Chemicals, Inc. OAPS as a mixture of isomers (meta:ortho:para = 60:30:10) was acquired from Mayaterials, Inc. (Ann Arbor, MI, USA). HPLC-grade *N*-methyl-2-pyrrolidinone (NMP) and pyridine were purchased from Sigma−Aldrich. Anhydrous acetic anhydride was purchased from Fisher Scientific. Dianhydrides were dried at 125 oC under vacuum for 24 h before use. All other reagents were used without further purification.

General. Attenuated total reflectance (ATR) infrared spectroscopy was obtained using a Nicolet Nexus 470 FT-IR spectrometer. Solid ^{13}C NMR spectroscopy was carried out with a Bruker Avance-300 spectrometer, using cross-polarization and magic angle spinning at 11 kHz. The solid ^{13}C spectra were externally referenced to the carbonyl of glycine (176.1, relative to tetramethylsilane (TMS)). Scanning electron microscopy (SEM) micrographs were obtained using a Hitachi S-4700 field-emission SEM system after sputter-coating the samples with gold. The samples were out-gassed at 80 °C for 8 h under vacuum before running nitrogen adsorption porosimetry with an ASAP 2000 surface area/pore distribution analyzer (Micromeritics Instrument Corp.). The skeletal density was measured using a Micromeritics Accupyc 1340 helium pycnometer. Using bulk density (ρ_b) and skeletal density (ρ_s) measured by helium pycnometry, the percent porosity was calculated using eq 1:

$$\text{porosity}\,(\%) = \left(1 - \frac{\rho_b}{\rho_s}\right) \times 100 \qquad (1)$$

Thermogravimetric analysis (TGA) was performed using a TA model 2950 HiRes instrument. Samples were examined at a temperature ramp rate of 10 °C/min from room temperature to 750 °C under nitrogen or air.

Preparation of OAPS Cross-Linked Polyimide Aerogel Monoliths. Polyimide aerogels were prepared as previously described.[10] Poly(amic acid) oligomer was synthesized in NMP using a molar ratio of dianhydride to total diamines of 26:25, which is formulated to provide oligomers with an average of 25 repeat units

dx.doi.org/10.1021/am301347a | ACS Appl. Mater. Interfaces 2012, 4, 5422−5429

Table 1. Process Variables and Properties of Polyimide Aerogels Prepared in the Study[a]

rigid diamine (%)	rigid diamine type	density (g/cm^3)	film density (g/cm^3)	surface area (m^2/g)	porosity (%)	shrinkage (%)	Young's modulus (MPa)	tensile modulus (MPa)	tensile stress at break (MPa)
100	PPDA	0.296	0.395	380	82.0	38.3	78.7	167.5	4.5
75	PPDA	0.267	0.400	362	83.4	36.4	54.3	155.0	3.9
50	PPDA	0.291	0.451	325	80.3	37.7	51.7	130.9	3.5
25	PPDA	0.206	0.274	335	85.8	29.5	20.2	72.2	1.6
0	PPDA	0.122	0.163	254	91.4	16.2	18.4	35.2	2.1
100	DMBZ	0.086	0.108	507	94.1	6.0	17.9	72.8	2.1
75	DMBZ	0.086	0.150	404	93.8	6.1	25.6	76.6	1.9
50	DMBZ	0.094	0.197	434	93.8	8.5	21.5	58.6	3.4
25	DMBZ	0.101	0.132	371	93.1	9.8	18.0	40.0	1.2
0	DMBZ	0.116	0.162	270	92.4	14.1	10.4	25.4	1.4
100	PPDA	0.268		413	85.3	36.9	56.0		
50	PPDA	0.214		385	86.2	31.2	26.7		
0	PPDA	0.133	0.166	292	91.4	19.0	23.9	33.7	1.2
100	DMBZ	0.089		489	93.9	6.7	22.1		
50	DMBZ	0.110	0.179	351	92.8	12.9	18.5	54.8	1.8
0	DMBZ	0.153	0.157	366	90.7	19.7	19.4	31.2	1.3

[a]ODA fraction is 100% − rigid diamine %.

terminated with anhydride. The mole percent of rigid diamine in place of ODA ranges from 0 to 100% in this study, as shown in Table 1. Since each OAPS contains eight amine groups, which can react with the two terminal anhydride groups on the poly(amic acid) oligomers, a ratio of four oligomers to one OAPS was used. The total weight of precursors in solution was formulated to be 10% w/w in all cases. A sample procedure for an oligomer made using 50% DMBZ and 50% ODA is as follows: To a stirred solution of DMBZ (0.443g, 2.09 mmol) and ODA (0.418 g, 2.09 mmol) in 17 mL NMP was added BPDA (1.278 g, 4.34 mmol). The mixture was stirred until all BPDA was dissolved, and a solution of OAPS (0.0481 g, 0.042 mmol) in 2.145 mL NMP was added. The resulting solution was stirred for 5 minutes, after which acetic anhydride (3.275 mL, 34.7 mmol) and then pyridine (2.81 mL, 34.7 mmol) were added, both representing an 8:1 ratio to BPDA. The solution was continually stirred for 10 min and then poured into a 20-mL syringe mold (2 cm in diameter), prepared by cutting off the needle end of the syringe and extending the plunger all the way out. The gels, which formed within 30 min, were aged in the mold for 1 day before extraction into fresh NMP to soak for 24 h, to remove acetic acid and pyridine. The solvent within the gels was then gradually exchanged to acetone in 24-h intervals starting with 75% NMP in acetone, followed by 25% NMP in acetone and, finally, three more times with 100% acetone. The gels were then placed in a 1-L supercritical fluid extraction chamber in acetone and washed with liquid CO_2 at ∼100 bar and ∼25 °C in four 2-h cycles. The chamber was then heated to 45 °C and the CO_2 was converted to a supercritical state. Gaseous CO_2 was slowly vented out at the rate of 4.5 m/h from the chamber over 3 h. The dry polyimide aerogels produced in this way have a density of 0.095 g/cm^3 and porosity of 93.7%. ^{13}C CPMAS NMR (ppm): 19.6, 124.3, 130.7, 143.9, 155, 165.9. FT-IR (cm^{-1}): 1775, 1715, 1596, 1498, 1417, 1370, 1236, 1170, 1112, 1088, 1008, 825, 736.

Procedure To Make Polyimide Aerogel Films. The same OAPS cross-linked polyamic acid solution as described above was cast onto a PET carrier, using a 12-in.-wide doctor blade at a speed of 80 cm/min. The gel film was peeled away from the carrier film. Afterward, the films were washed in 24-h intervals in 75% NMP in acetone, followed by 25 % NMP in acetone and finally washed three more times with acetone. Supercritical drying was carried out as described previously to give polyimide aerogel thin films.

Mechanical Characterization. The specimens were cut and polished to make sure that the top and bottom surfaces were smooth and parallel. Samples were conditioned at room temperature for 48 h prior to testing. The diameter and length of the specimens were measured before testing. The specimens were tested in accordance with ASTM Standard D695-10, with the sample sizes nominally 1.5−1.8 cm in diameter and 3 cm in length (close to the 1:2 diameter-to-length ratio prescribed for the testing of polymer foams). The samples were tested between a pair of compression plates on a Model 4505 Instron load frame using the Series IX data acquisition software. All testing was carried out under nominal room conditions, and at a crosshead speed of 0.05 in./min, as dictated by the ASTM guidelines. The aerogels were crushed to 75% strain or the full capacity of the load cell (whichever occurred first). The Young's modulus was taken as the initial linear portion of the slope of the stress strain curve.

The thin films were cut into 5 mm × 33 mm strips and tested at an extension speed of 2 mm/min and 100N load using a Model 5567 Instron Tensile Test Machine with Bluehill software. A film strip was fixed on a rectangular cardboard frame by adhering the two ends with cellophane tape. The center part of the cardboard was open to expose the test area of the sample. This setup was used to support and align the flexible film to be straight for installation on the machine clip. The edges of the cardboard frame were cut before testing. The tensile modulus was taken as the initial linear portion of the slope of the stress−strain curve.

Statistical Analysis. Experimental design and analysis was conducted using Design Expert Version 8.1, available from Stat-Ease, Inc. (Minneapolis, MN, USA). Multiple linear regression analysis was used to derive empirical models to describe the effect of each of the process variables studied on measured properties. A full quadratic model including all main effects, second-order effects, and all two-way interactions was entertained, and continuous variables were orthogonalized (transformed to −1 to +1 scale) before analysis. Terms deemed to not be significant in the model (<90 % confidence) were eliminated one at a time using a backward stepwise regression technique.

RESULTS AND DISCUSSION

Process variables and properties of the polyimide aerogels prepared in the study are summarized in Table 1. Polyimide aerogels were made using 10 w/w % solutions of precursors in NMP, with equivalent ratios of dianhydride to total diamines of 26:25 upon mixing. Amber-colored poly(amic acid) oligomers with terminal anhydride groups were formed in solution. As expected, the terminal anhydride groups reacted with the amines of OAPS, after which pyridine (to catalyze imidization) and acetic anhydride (to scavenge water bi-product of condensation) were added to the solution (pH of the solution is ∼6.0). The resulting polyimide aerogels differ slightly in color, depending on the formulation. For example, aerogels made using PPDA as the diamine are orange, while those made

from DMBZ are light yellow and those made from ODA are slightly darker yellow. To some extent, the differences in color reflect different densities produced using the different diamines: PPDA, having the highest density, has the most intense color, followed by ODA, then DMBZ. OAPS cross-linked aerogels made from 100% PPDA gel the fastest, with 10% w/w solutions having a gelation time of ~5 min. Other formulations gel within 30 min. Thin films of OAPS cross-linked polyimide aerogels were fabricated as previously described. The thickness of the film is determined by the gap between the carrier film and the doctor blade, the solution viscosity, the casting speed, and the head pressure, as well as the shrinkage. Solutions made using PPDA were the most viscous, while those made using DMBZ and/or ODA were slightly less viscous. With a casting speed of 80 cm/min and a 12-in.-wide doctor blade with a gap of 1.09 mm, the films have a thickness of nominally 0.3−0.7 mm.

Fourier tranform infrared (FT-IR) spectra, as seen in Figure 1, of all of the aerogels in the study contain characteristic bands for polyimides, including 1370 cm^{-1} (υ imide C−N), 1715 cm^{-1} (symmetric υ imide C═O) and 1775 cm^{-1} (asymmetric υ imide C═O). A band at ~1860 cm^{-1}, which would indicate the existence of unreacted anhydride, is not observed. In addition, bands at ~1660 cm^{-1} (υ amic acid C═O) and ~1535 cm^{-1} (υ amide C−N) are absent, further indicating that imidization is complete. Bands at ~1807 cm^{-1} and 980 cm^{-1}, expected for the isoimide structure, also are not observed in the FTIR spectra. The bands at 1112 cm^{-1} and 1088 cm^{-1} are attributed to the vibration of Si−O−Si from OAPS.

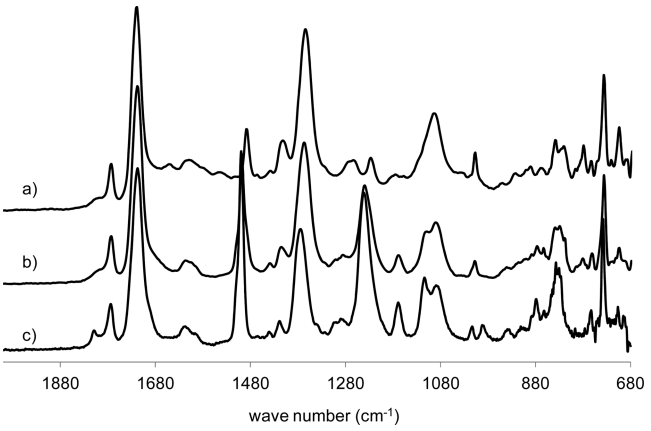

Figure 1. FT-IR spectra of polyimide aerogels made with (a) 100% DMBZ, (b) 50% DMBZ/50% ODA, and (c) 100% ODA.

As shown in Figure 2, the ^{13}C NMR spectra from solid samples of polyimide aerogels all contain an imide carbonyl peak at ~165 ppm, and aromatic peaks between 115 ppm and 140 ppm. Polyimide aerogels made using ODA (Figures 1b and 1c) have a peak at 153 ppm, corresponding to the aromatic ether carbon. Increasing the fraction of ODA increases the relative intensity of the 153 ppm peak. NMR spectra of polyimide aerogels made with DMBZ (Figure 1a) have a characteristic aliphatic peak at 19 ppm for the pendant methyl groups, which increases with increasing DMBZ content.

As seen in Figure 3a, the diamine combination has a strong influence on the shrinkage (standard deviation = 2.33%, R^2 = 0.98) occurring during fabrication of the aerogels. Overall, OAPS cross-linked polyimide aerogels exhibit slightly lower shrinkage than those previously reported using TAB as a cross-linker,[9] resulting in slightly lower densities and higher porosities. However, trends due to diamine are the same, whether OAPS or TAB is the cross-link, with the most shrinkage exhibited in aerogels made using PPDA and the least shrinkage with DMBZ. As previously discussed,[9] since this shrinkage occurs mostly during gelation, this difference is most likely due to a combination of solvent interactions, chain rigidity, and chain packing. PPDA and DMBZ are both rigid diamines, but DMBZ, with a 75° torsional angle between phenyl rings, prevents polymer chains from packing close together. As shown in Figure 3a, polyimide aerogels made using ODA shrink ~15% during processing, while replacing ODA with increasing amounts of DMBZ slightly reduces shrinkage.

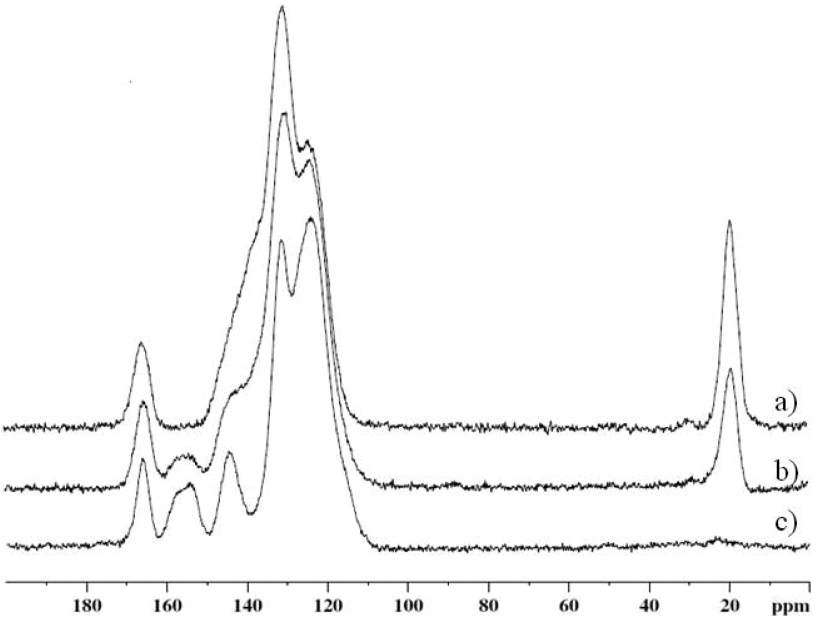

Figure 2. ^{13}C solid-state NMR spectra of polyimide aerogels made with (a) 100% DMBZ, (b) 50% DMBZ/50% ODA, and (c) 100% ODA.

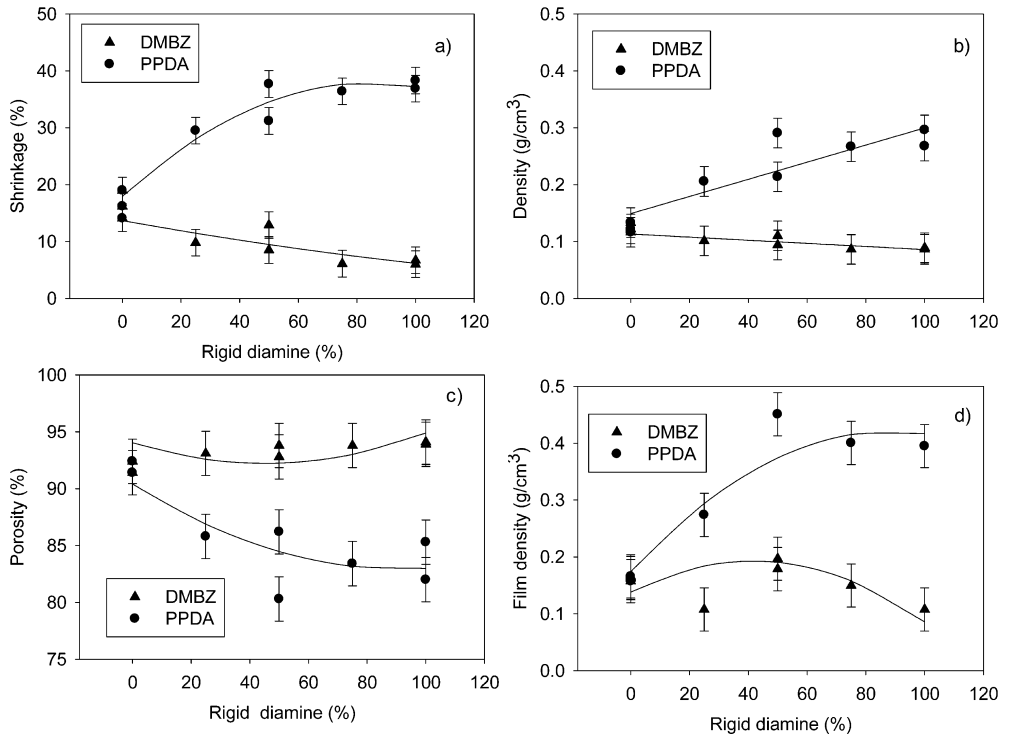

Figure 3. Graphs of (a) shrinkage, (b) density of polyimide aerogel cylinders, (c) porosity of the polyimide aerogels, and (d) density of the polyimide aerogel films made using ODA, PPDA, and DMBZ. Rigid diamine = % DMBZ or PPDA. Error bars represent one standard deviation from fitted models.

Increasing the concentration of PPDA in the aerogels greatly increases shrinkage, with aerogels containing at least 50% PPDA shrinking more than 30%. As shown in Figure 3b, densities of the polyimide aerogels (standard deviation = 0.026 g/cm^3, R^2 = 0.92) follow the same trends as shrinkage, with densities decreasing slightly with increasing DMBZ fraction, and greatly increasing with increasing PPDA fraction. As expected, porosity (standard deviation = 1.95%, R^2 = 0.89), shown in Figure 3c, increases as density and shrinkage decrease, with aerogels derived from DMBZ being the most porous (up to 94%). As seen in Figure 3d, the density of the films (standard deviation = 0.038 g/cm^3, R^2 = 0.93) are higher than those of the cylindrical samples, which may due to more solvent evaporation from the larger exposed surface area of the gel films during the casting process.

The surface areas and pore volume of the monoliths were measured by nitrogen sorption, using the Branuaer–Emmett–Teller (BET) method.[14] BET surface areas of the aerogels (standard deviation = 30.99 m^2/g, R^2 = 0.86) ranged from 250 m^2/g to over 500 m^2/g, depending on the diamine used, and were similar to trends previously observed with TAB as the cross-link.[9] As seen in Figure 4a, polyimide aerogels made using just ODA have the lowest surface area. As seen in Figure 4a, replacing ODA with either PPDA or DMBZ increases the surface area over the entire range, with DMBZ increasing the surface area more than PPDA. The nitrogen sorption isotherms for all of the polyimide aerogels are IUPAC Type IV curves with an H1 hysteresis loop, indicating that the monoliths consist predominately of three-dimensional (3D) continuous mesopores/macropores.[15] A graph of relative pore volume versus pore diameter for selected formulations is shown in Figure 4b. According to the IUPAC definition, pores are classified by the pore diameter, with micropores having

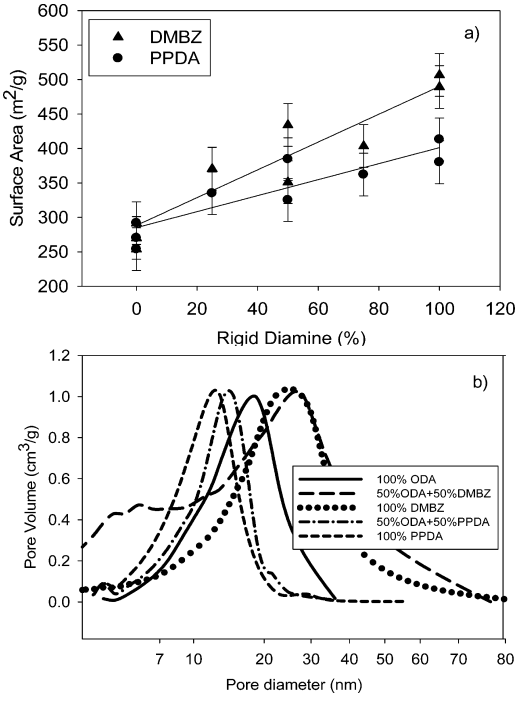

Figure 4. (a) Surface area of the polyimide aerogels made with varying amounts of ODA with PPDA or DMBZ; (b) relative pore volume versus pore diameter of the polyimide aerogels with 100% ODA, 50% DMBZ + 50% ODA, 100% DMBZ, 50% PPDA + 50% ODA, and 100% PPDA. Error bars represent one standard deviation from fitted models.

diameters less than 2 nm, mesopores having diameters between 2 and 50 nm, and macropores having pore diameters larger than 50 nm. From Figure 4b, it can be seen that the aerogels

dx.doi.org/10.1021/am301347a | ACS Appl. Mater. Interfaces 2012, 4, 5422–5429

have pore diameters in the range of mesopores to macropores, with the distribution peaking at ~14−30 nm. Aerogels made using only PPDA have the smallest pore diameter, most likely because they have the highest shrinkage, while those made using only DMBZ have the largest pore diameters and the smallest shrinkage. Aerogels made using only ODA have a pore size distribution that falls between those made with PPDA and DMBZ.

Field-emission scanning electron microscopy (FESEM) micrographs of the selected polyimide aerogel formulations made in cylinder form are shown in Figures 5a−e. Unlike silica

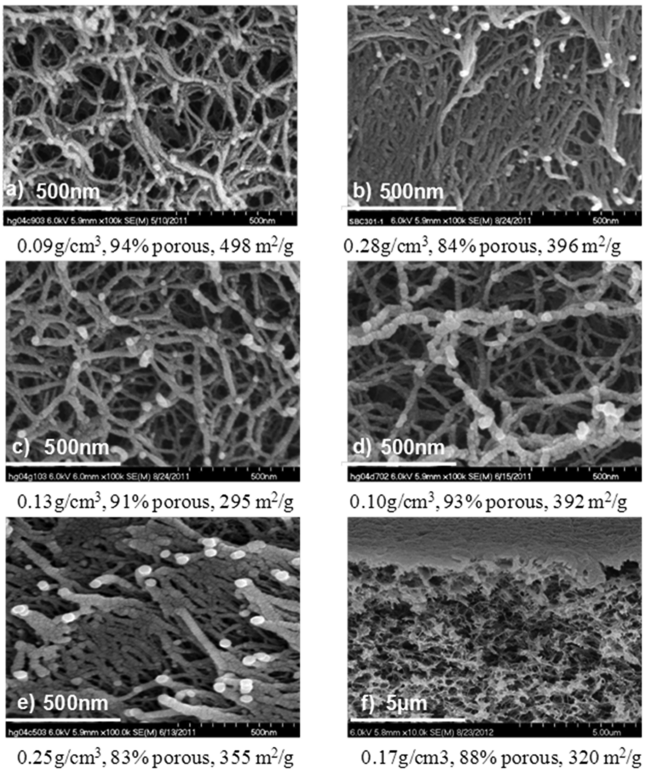

Figure 5. FESEM of the polyimide areogels with (a) 100% DMBZ, (b) 100% PPDA, (c) 100% ODA, (d) 50% DMBZ + 50% ODA, (e) 50% PPDA + 50% ODA, and (f) cross section of aerogel film with 50% DMBZ + 50% ODA. Related density, porosity, and surface area are listed under the images.

aerogels, the polyimide aerogels consist of a 3D network of polymer nanofibers tangled together, with fiber diameters ranging from 15 nm to 50 nm. This arrangement of nanofibers most likely forms during polymerization and subsequent gelation, with influence from solvent interaction. Aerogels made using PPDA as the diamine have densely packed strands (Figure 5b). This may be due to the polyimide oligomers having greater chain rigidity, high planarity, and shorter chain length between cross-links, leading to greater shrinkage during processing. This is in contrast to aerogels made using either DMBZ as the diamine (Figure 5a), ODA as the diamine (Figure 5c), or a combination (Figure 5d), which have more open porosity around the fiber strands. Aerogels made with 50/50 mixtures of PPDA and ODA (Figure 5e) resemble the structure of the 100% PPDA aerogels, with similar shrinkage and density. Figure 5f shows the cross-section of a polyimide aerogel film made using a 50/50 mixture of DMBZ and ODA. Because of the solvent evaporation in the casting process, the surface of the film appears denser, but the interior of the film has a fiberlike structure similar to the thicker cylindrical samples.

TGA of the OAPS cross-linked polyimide aerogels was performed in nitrogen from room temperature to 750 °C. Graphs of selected TGA curves are shown in Figure 6. For all

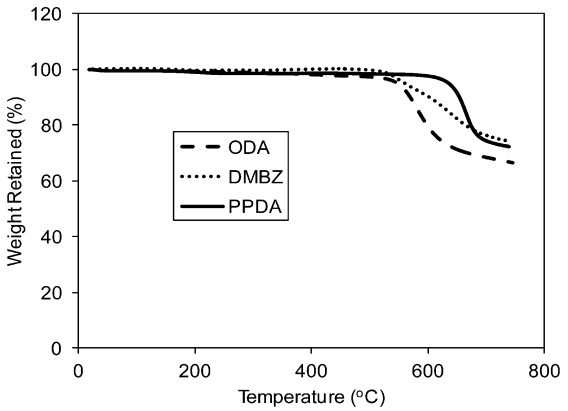

Figure 6. Thermogravimetric analysis (TGA) curves in N_2 of the polyimide aerogels made using DMBZ, PPDA, and ODA.

formulations, little weight loss occurs until the onset of the decomposition temperature at 525−625 °C, indicating that imidization is complete and NMP is removed completely by solvent exchange to acetone and supercritical drying. As previously reported with TAB cross-linked aerogels,[9] the onset of decomposition temperature varies with the diamine used, with the highest onset of decomposition seen for the formulations made using PPDA. Formulations made using DMBZ have the lowest decomposition temperature, because of the loss of the pendant methyl groups from DMBZ. All of the formulations have a char yield in nitrogen above 70%. These results are in general agreement with the thermal studies of nonporous, bulk-form polyimide.[16−18]

Compression tests were performed on all aerogel formulations in the study. Young's modulus (standard deviation (log) = 0.11, R^2 = 0.85) of the aerogels was measured as the initial slope of the stress−strain curves and is plotted in Figure 7. Similar to TAB cross-linked polyimide aerogels, OAPS cross-linked polyimide aerogels made using PPDA as the diamine exhibit higher modulus than those made with DMBZ. As seen in Figure 7, the modulus of the polyimide aerogel increases as the fraction of rigid diamine increases. Generally, in aerogels, the modulus increases as the density increases.[19] Aerogels made using PPDA follow this same trend, with the modulus and density both increasing with increasing PPDA content. Surprisingly, Young's modulus of aerogels made using DMBZ increases slightly with increasing DMBZ content, while the density, as previously shown in Figure 3b, actually decreases slightly. This could be due to slight differences in the cure state, although no differences among the formulations were detected. Most likely, the increase in modulus is due to the greater rigidity of the polymer backbone. In any case, it is possible to fabricate a polyimide aerogel with both low density and high modulus by increasing the ratio of DMBZ in the aerogel structure.

The tensile modulus (standard deviation (log) = 0.048, R^2 = 0.98) and tensile stress (standard deviation (log) = 0.084, R^2 = 0.87) of the polyimide aerogel films with rigid diamine varying

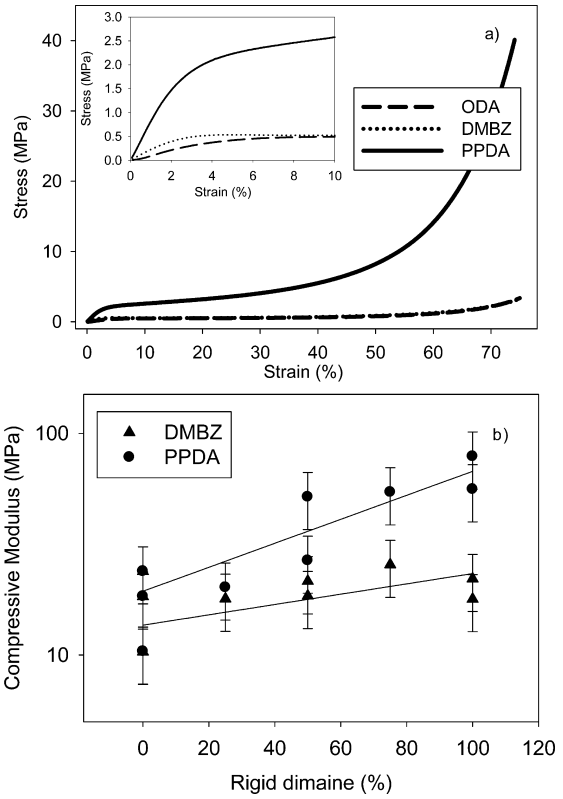

Figure 7. Graph of (a) stress–strain curves of polyimide aerogels made using DMBZ, PPDA, and ODA; (b) graph of Young's modulus for polyimide aerogels made using ODA with varying amounts of DMBZ or PPDA. Error bars represent one standard deviation from fitted models.

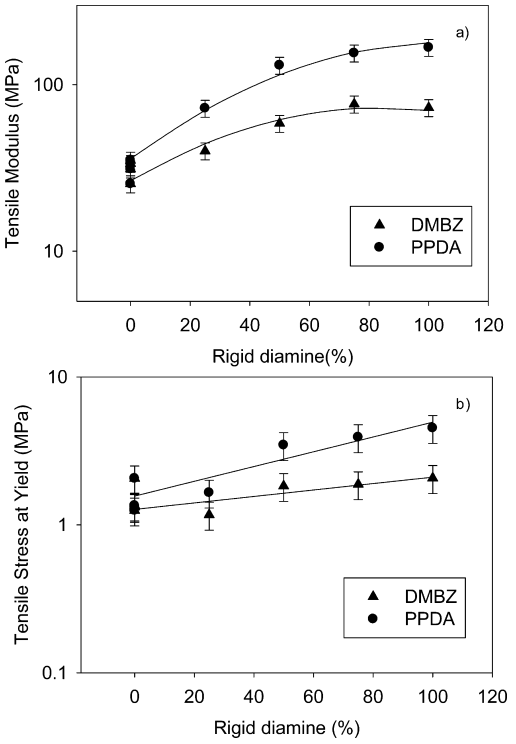

Figure 8. Graphs of (a) tensile modulus and (b) tensile stress at break of polyimide aerogel films made using ODA with varying amounts of DMBZ or PPDA. Error bars represent one standard deviation from fitted models.

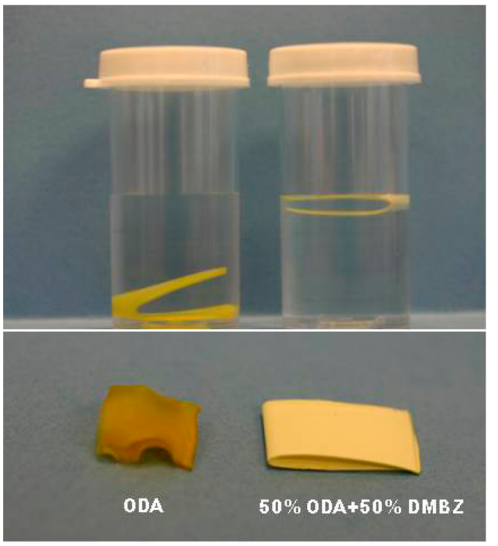

Figure 9. Polyimide aerogel thin film made using 100% ODA (left) and 50% DMBZ + 50 % ODA (right) shown in water (top) and after air drying (bottom).

from 0% to 100%, as shown in Figure 8. Generally, the tensile modulus should be similar to the compressive modulus. The higher tensile modulus observed in the testing may be attributed to the higher density of the films. Similar to compression, tensile modulus and tensile stress at break of the aerogel films greatly increases with increasing PPDA content, which is consistent with the concomitant increase in density. Aerogel films made using DMBZ again show an increase in modulus and tensile stress at break while the density is actually decreasing, leading to stronger aerogels at lower density. The tensile modulus is comparable to that previously reported for the same formulations of TAB cross-linked aerogels. However, the TAB aerogels generally have a higher stress at break than the OAPS cross-linked aerogels.

Films from all formulations were soaked in water for 24 h and later dried in air to test the moisture resistance. As seen in Figure 9, samples made using 100% ODA absorbed water into the pores and sank to the bottom after a short time. This was also true for samples made with 75% ODA and 25% DMBZ, or any amount of PPDA. However, aerogels made with at least 50% DMBZ were water-resistant, as shown in Figure 8, and remained floating on the surface of the water indefinitely. Those aerogels that absorbed water tended to shrivel upon air drying. The aerogels made with at least 50% DMBZ were unchanged. Water contact angle measurements of these polyimide aerogel films made with 50%–100% DMBZ ranged from 85° to 90°. It is surprising that the aerogels made using PPDA are not moisture-resistant, since the phenyl ring is also hydrophobic. This may be due to the ratio and distribution of hydrophobic and hydrophilic groups in the polymer backbones. Hence, the smaller size and planar nature of the hydrophobic phenyls in PPDA oligomers may not be enough to shield the hydrophilic imide rings. Films fabricated with 100% DMBZ are the most brittle among all the films, while formulations made using at least 50% ODA were quite flexible. As seen in Figure 9, thin films of aerogels made using 50% DMBZ are flexible enough to bend back nearly 180° without cracking or flaking

dx.doi.org/10.1021/am301347a | ACS Appl. Mater. Interfaces 2012, 4, 5422–5429

and maintain this flexibility after being soaked in water and dried in air.

CONCLUSIONS

A series of polyimide aerogels was synthesized using BPDA and combinations of different diamines (two rigid and one flexible), and cross-linked using octa-aminophenyl decorated polysilsesquioxane (OAPS). The resulting aerogels vary in density, shrinkage, porosity, surface area, and modulus, depending on the types of diamines, and the proportions of rigid diamine to flexible diamine used. Using OAPS as the cross-link slightly leads to lower shrinkage and lower density, compared to aerogels previously reported using TAB as the cross-link. However, similar to TAB cross-linked aerogels, aerogels made using DMBZ have lower density but also higher porosity and surface area. With the onset of decomposition at 500 °C and higher, all formulations are quite stable and also exhibit high char yield in nitrogen. Increasing the rigid diamine fraction results in increased tensile and compressive modulus of the aerogels. It is interesting to note that, for aerogels made with increasing DMBZ fraction, this increase in modulus occurs even though the density is decreasing. Using at least 50% DMBZ in the formulations also results in good moisture resistance in the polyimide aerogels, which is a key attribute for employing these aerogels as insulation in many instances. Thus, a formulation made using 50% DMBZ and 50% ODA results in the best combination of moisture resistance, flexibility, low density, good thermal stability, and excellent mechanical properties. Thermal conductivity measurements of the aerogels are underway.

AUTHOR INFORMATION

Corresponding Author

*E-mail addresses: haiquan.n.guo@nasa.gov (H.G.), maryann.meador@nasa.gov (M.A.B.M.).

Notes

The authors declare no competing financial interest.

ACKNOWLEDGMENTS

We gratefully acknowledge support from the Fundamental Aeronautics Program (Hypersonics). We also thank Daniel A. Scheiman, Zin Technologies, Inc., for carrying out porosimetry and thermal analysis; Baochau N. Nguyen, Ohio Aerospace Institute, for NMR spectra; and Anna Palczer, for nitrogen sorption experiments. We also thank the Third Frontier Program of the State of Ohio for funding the construction of the roll-to-roll film manufacturing line.

REFERENCES

(1) Hüsing, N.; Schubert, U. *Angew. Chem., Int. Ed.* **1998**, *37*, 22−45.
(2) Moner-Girona, M.; Roig, A.; Molins, E.; Martínez, E.; Esteve, J. *J. Appl. Phys. Lett.* **1999**, *75*, 653−655.
(3) Tang, H. H.; Orndoff, E. S.; Trevino, L. A. Presented at the *International Conference On Environmental Systems Technical Papers*, Paper No. 2006-01-2235.
(4) Braun, R. D.; Manning, R. M. *J. Spacecr. Rockets* **2007**, *44*, 310−323.
(5) Smith, B. P.; Tanner, C. L.; Mahzari, M.; Clark, I. G.; Braun, R. D.; Cheatwood, F. M. Presented at the *2010 IEEE Aerospace Conference*, Big Sky, MT, ; IEEE: Piscataway, NJ, 2010; Paper No. IEEEAC 1276.
(6) Smith, B.P.; Clark, I.G.; Braun, R.D Presented at the *2011 IEEE Aerospace Conference*, Big Sky, MT ; IEEE: Piscataway, NJ, 2011; Paper No. IEEEAC 1312.
(7) Miller, S.; Leventis, N.; Johnston, J. C.; Meador, M. In *Proceedings of the National Space and Missile Materials Symposium*, Summerlin, NV, June 2005.
(8) Randall, J. P.; Meador, M. A. B.; Jana, S. C. *ACS Appl. Mater. Interfaces* **2011**, *3*, 613−626.
(9) Meador, M.A.B.; Malow, E. J.; Silva, R.; Wright, S.; Vivod, S. L.; Guo, H. *ACS Appl. Mater. Interfaces* **2012**, *4*, 536−544.
(10) Guo, H.; Meador, M. A. B.; McCorkle, L.; Quade, D. J.; Guo, J.; Hamilton, B.; Cakmak, M.; Sprowl, G. *ACS Appl. Mater. Interfaces* **2011**, *3*, 546−552.
(11) Rhine, W.; Wang, J.; Begag, R. *Polyimide aerogels, carbon aerogels, and metal carbide aerogels and methods of making same*. U.S. Patent 7074880 B2, 2006.
(12) Chidambareswarapatter, C.; Larimore, Z.; Sotiriou-Leventis, C.; Mang, J. T.; Leventis, N. *J. Mater. Chem.* **2010**, *20*, 9666−9678.
(13) Del Corso, J. A.; Cheatwood, F. M.; Bruce, W. E.; Hughes, S. J.; Calomino, A. M. Presented at the *21st AIAA Aerodynamic Decelerator Systems Technology Conference and Seminar*, Dublin, Ireland, May 23−26, 2011; AIAA: Reston, VA, 2011, Paper No. 2510.
(14) Brunauer, S.; Emmett, P. H.; Teller, E. *J. Am. Chem. Soc.* **1938**, *60*, 309−319.
(15) Barton, T. J.; Bull, L. M.; Klemperer, W. G.; Loy, D. A.; McEnaney, B.; Misono, M.; Monson, P. A.; Pez, G.; Scherer, G. W.; Vartuli, J. C.; Yaghi, O. M. *Chem. Mater.* **1999**, *11*, 2633−2656.
(16) Hergenrother, P. M. *High Perform. Polym.* **2003**, *15*, 3−45.
(17) For example, see: Ehlers, G. F. L., Soloski, E. J. *Thermal Analysis of Polymers in Air*; Technical report AFML-TR-78-64; Air Force Materials Laboratory: Wright-Patterson AFB, OH, 1978.
(18) Dine-Hart, R. A.; Wright, W. W. *Makromol. Chem.* **1972**, *153*, 237−254.
(19) Pekala, R.W.; Hrubesh, L. W.; Tillotson, T. M.; Alviso, C. T.; Poco, J. F.; LeMay, J. D. *Mater. Res. Soc. Symp. Proc.* **1991**, *207*, 197.

NOTE ADDED AFTER ISSUE PUBLICATION

This paper was published on the Web on September 20, 2012, with incorrect text at the beginning of the last paragraph on page 5427 that was due to a production error. The corrected version was reposted on December 7, 2012.